Materials Science and Engineering C 33 (2013) 4295–4304

Contents lists available at ScienceDirect

Materials Science and Engineering C

journal homepage: www.elsevier.com/locate/msec

Systematic study of alginate-based microcapsules by micropipette aspiration and confocal fluorescence microscopy

Rachelle M. Kleinberger [a], Nicholas A.D. Burke [a], Kari Dalnoki-Veress [b], Harald D.H. Stöver [a,*]

[a] Department of Chemistry and Chemical Biology, McMaster University, 1280 Main Street West, Hamilton, Ontario L8S 4M1,Canada
[b] Department of Physics and Astronomy, McMaster University, 1280 Main Street West, Hamilton, Ontario L8S 4M1,Canada

ARTICLE INFO

Article history:
Received 4 April 2013
Received in revised form 9 May 2013
Accepted 19 June 2013
Available online 28 June 2013

Keywords:
Alginate capsules
Poly-L-lysine
Micropipette aspiration
Mechanical properties
Membrane thickness

ABSTRACT

Micropipette aspiration and confocal fluorescence microscopy were used to study the structure and mechanical properties of calcium alginate hydrogel beads (**A** beads), as well as **A** beads that were additionally coated with poly-L-lysine (**P**) and sodium alginate (**A**) to form, respectively, **AP** and **APA** hydrogels. **A** beads were found to continue curing for up to 500 h during storage in saline, due to residual calcium chloride carried over from the gelling bath. In subsequent saline washes, micropipette aspiration proved to be a sensitive indicator of gel weakening and calcium loss. Aspiration tests were used to compare capsule stiffness before and after citrate extraction of calcium. They showed that the initial gel strength is largely due to the calcium alginate gel cores, while the long term strength is solely due to the poly-L-lysine–alginate polyelectrolyte complex (PEC) shells. Confocal fluorescence microscopy showed that calcium chloride exposure after PLL deposition led to PLL redistribution into the hydrogel bead, resulting in thicker but more diffuse and weaker PEC shells. Adding a final alginate coating to form **APA** capsules did not significantly change the PEC membrane thickness and stiffness, but did speed the loss of calcium from the bead core.

1. Introduction

Encapsulation of genetically engineered therapeutic cells has been proposed for treatment of several enzyme and hormone deficiency disorders, including diabetes [1], Parkinson's [2], and lysosomal storage disorders [3]. Encapsulation of allogeneic cells in a semi-permeable membrane can provide physical immune protection, and may enable long-term delivery of therapeutic peptides. The most common approach to cell encapsulation involves embedding cells in a calcium alginate bead that is then coated with a polycation, commonly poly-L-lysine (PLL), to form a stable polyelectrolyte complex (PEC) shell to increase the stability, and tune the permeability, of the membrane [4].

These beads are usually further coated with alginate in order to hide the PLL from the host's immune system, resulting in capsules known as alginate/PLL/alginate or **APA** capsules [4]. A recent study by Tam et al. suggests that the final layer of alginate does not significantly alter the outer composition of the membrane, casting doubt on the need for this final alginate coating [5].

The properties of **APA** capsules depend significantly on the type and concentration of alginate, PLL and gelling ion (typically calcium) used, as well as on the protocols used for their preparation and storage. Capsules can fail in their immune-protective role in a number of ways, which may include mechanical rupture, loss of the outer alginate coating followed by fibrotic overgrowth [6], and even degradation of alginate by redox processes or hydrolysis [7].

A key issue is the loss of calcium through exchange with, *e.g.*, sodium [8–10], leading to bead swelling [10], decreased gel modulus [11], and even rupture of the **APA** membrane [4].

Improved understanding and control of capsule properties are key challenges in the field, and have led to calls for greater standardization between different labs [12]. Many novel approaches to create covalently crosslinked capsules still use calcium alginate and polycations, such as PLL [13–16].

Tissue-like capsule stiffness and long-term mechanical integrity [17] are critical for successful transplantation of encapsulated therapeutic cells, as well as for related use of these gels in stem cell differentiation and regenerative medicine [18–21].

The mechanical stability of **APA**-type capsules has often been studied using ensemble pass/fail screening for the fraction of intact capsules following exposure to hypotonic media [15,22], or shaking with glass beads [23]. The thickness of the membrane formed by the PLL–alginate PEC has been used to indicate capsule strength in some studies [4,24] though at times the strongest capsules were reported to be those having a thin shell formed using higher molecular weight (MW) PLL [24]. In other studies, swelling ratios were used as an indicator of strength [4,25].

Mechanical tests of single alginate capsules have been carried out using atomic force microscopy (AFM) [26], compression testing

Abbreviations: PEC, polyelectrolyte complex; PLL, poly-L-lysine; **A**, alginate; **AP**, alginate/poly-L-lysine; **APA**, alginate/poly-L-lysine/alginate; MW, molecular weight; G, guluronic acid; M, mannuronic acid.

* Corresponding author. Tel.: +1 9055259140x24983.
E-mail address: stoverh@mcmaster.ca (H.D.H. Stöver).

0928-4931/$ – see front matter © 2013 Published by Elsevier B.V.
http://dx.doi.org/10.1016/j.msec.2013.06.033

[11,17,27–32], rheology [11], and deformation by centrifugal forces [33,34]. AFM measurements mainly provide information about local surface properties [26], while compression tests provide information about the whole bead from the analysis of Young's modulus [30], viscoelastic properties [35,36], and bursting forces [17,36,37].

Micropipette aspiration is a common technique for studying mechanical properties of cells [38–40] and small semi-permeable capsules [41–44]. The application of this method to larger, alginate-based capsules is rare, despite the simplicity of the technique and the quantitative information that can be extracted. Hunkeler and co-workers made limited use of aspiration to measure the membrane tension of capsules composed of an alginate/cellulose sulfate core coated with polymethylene-co-guanidine [45].

This paper describes a simple yet sensitive aspiration-based test of capsule stiffness, its validation and use to study the properties of model capsules as a function of preparation and storage conditions. Confocal microscopy was used to determine capsule morphology, in particular shell thickness, through the use of fluorescein labeled PLL.

2. Experimental

2.1. Materials

Sodium alginate (Pronova UP MVG, batch: BP-0908-01) was purchased from Novamatrix (Sandvika, Norway). Poly-L-lysine hydrobromide (PLL, M_n 15–30 kDa), fluorescein isothiocyanate (FITC) and HEPES sodium salt from Sigma-Aldrich (Oakville, ON Canada), and sodium chloride and calcium chloride from Caledon Laboratories (reagent grade, Georgetown, ON), were used as received. Trisodium citrate dihydrate (AnalaR) was purchased from EMD Chemicals (Gibbstown, NJ, USA) and was used as received. Sodium hydroxide and hydrochloric acid stock solutions (0.1 or 1.0 M) were purchased from LabChem (Pittsburgh, PA, USA).

2.2. PLL fluorescent labeling

FITC-labeled PLL, PLL*f*, was prepared as described earlier [16]. Briefly, PLL (HBr form, 99.5 mg, 0.48 mmol lysine) was dissolved in 0.2 M $NaHCO_3$ buffer (pH 9) and 1.0 mg (0.0026 mmol) of FITC dissolved in N,N-dimethylformamide was added. The PLL*f* was purified by dialysis and isolated by freeze-drying (64.5 mg, 82% HCl form) with a labeling degree of 0.61%, determined from the maximum absorbance at 495 nm, using the absorption coefficient of free FITC of 77,000 $M^{-1}\,cm^{-1}$ [46]. The extinction coefficient of PLL*f*, was 2.67 $mL\cdot cm^{-1}\cdot mg^{-1}$, measured at 495 nm.

2.3. Preparation of calcium alginate beads (**A** beads)

A solution of sodium alginate (5–10 mL, 1 wt.%) in saline was filtered (0.2 μm) and then extruded into 60 mL of gelling bath consisting of de-ionized water containing 1.1 wt.% $CaCl_2$ (100 mM) and 0.45 wt.% NaCl (77 mM), reflecting a 12–24 molar excess of Ca^{2+} over carboxylates. Extrusion was done at a rate of 0.5 mL/min, using a syringe pump and a flat-tipped 27 G needle fitted inside a 1 mm diameter tube that provided an annular airflow of 3–4 L/min. This airflow was adjusted to generate narrow disperse calcium alginate beads (**A** beads) with mean diameters of 500 to 600 μm, and standard deviations of about 50 μm. After extrusion was complete, the beads were kept in the gelling bath for another 10 min before being transferred into fresh gelling bath solution (using a 3:10 volume ratio of settled bead suspension to wash solution) for an additional 10 min, and before moving on to coating or aging experiments as described below. All solutions were pre-cooled to 4 °C and the gelling bath was placed in an ice bath during bead formation. The beads have smooth surfaces, and equatorial/axial aspect ratios not exceeding 1.1.

2.4. Preparation of **AP** and **APA** capsules

AP beads were prepared by adding 10 mL of 0.05 wt.% PLL or PLL*f* in saline (pH 7.0–7.5) to 3.0 mL of settled, freshly prepared **A** beads. After 6 min with occasional swirling, the supernatant was removed, and the as-formed beads washed a) once with fresh gelling bath and once with saline or b) twice with saline. Each wash took 2 min unless stated otherwise. Supernatant from coating and washing steps were analyzed for residual PLL*f* content using UV/Vis.

APA capsules were prepared by adding 1.67 mL of 0.03% sodium alginate to 0.5 mL of settled **AP** beads for 4 min, with occasional swirling. The resulting **APA** capsules were washed twice with saline for 2 min. All washing steps involved a 3:10 volume ratio of settled beads to coating/washing solution.

2.5. Monitoring the effects of storage/washing conditions on **A** and **AP** beads

Freshly prepared **A** beads and **AP** capsules were stored in saline (154 mM NaCl) at 4, 20 and 40 °C. All washing steps used a volume ratio of settled beads to washing solution of 3:10. Beads were monitored by microscopy and aspiration at room temperature, in a small amount of their own supernatant. Supernatants were monitored for Ca^{2+} content using ICP-MS.

2.6. Citrate treatment

Sodium citrate (5 mL, 70 mM) and settled **AP** or **APA** capsules (0.5 mL) were mixed at room temperature for 5 min before the supernatant was removed and the settled, liquid filled capsules were washed once with saline (1.67 mL).

2.7. Micropipette aspiration (*Scheme* **1**)

A borosilicate disposable micropipette with an inner diameter of 290 μm and an outer diameter of 1120 μm (Fisher Scientific) was attached to a 10 mL glass buret (0.5 cm inner diameter, 65 cm length) using flexible Tygon tubing, forming a U-tube filled with water. A number of capillary tips from one batch were examined by optical or scanning electron microscopy (TESCAN VP SEM) and were found to have smooth, circular openings and near identical inner diameters of 291 ± 2 μm.

A syringe pump (NE-1600, New Era Pump Systems™) connected to the Tygon tubing *via* a Y-shaped connector allowed automated control of the height of the water column and hence the pressure differential. About 0.25–0.50 mL of a suspension of capsules in their own storage supernatant (unless indicated otherwise) was placed on a

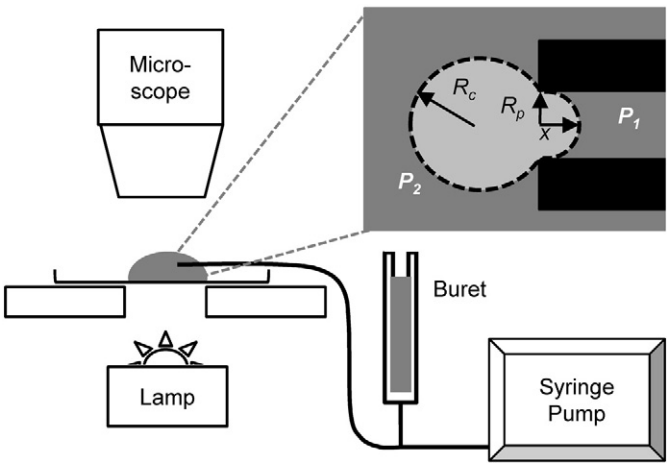

Scheme 1. Setup for micropipette aspiration.

flat, hydrophobic polystyrene dish located on the stage of an Olympus BH2-UMA optical microscope. Capsules were captured on the open end of the capillary while applying a negative pressure differential of 0.75 nN/μm^2 (equivalent to 0.75 kPa). Once a capsule was captured, the water column was lowered to 3.75 kPa at a rate of 0.75 kPa/min. The rate of change of applied pressure differential was constant for all capsules aspirated, allowing for direct comparison between the viscoelastic beads and capsules. Images of the aspirated capsule were taken every minute in transmission mode. The length of projection of the capsule into the capillary was measured using ImageJ software and plotted against the pressure differential. Measurements were conducted in triplicate, using a new capsule for each aspiration series.

2.8. Microscopy

Optical and fluorescence images of capsules were collected with an Olympus BX51 microscope equipped with a Q-Imaging Retiga EXi camera and ImagePro software. Average capsule diameters were determined from measurements of a minimum of 60 capsules.

Confocal microscopy images of **AP** or **APA** capsules prepared using PLL*f* were obtained with a Zeiss LSM510 confocal laser scanning microscope equipped with argon and HeNe lasers, operated with Zeiss LSM510 software, or on a Nikon Eclipse 90i upright microscope equipped with a Nikon C2 confocal head, an argon multi-line laser and NIS-Elements viewer software. The extent of PLL*f* diffusion into the capsules, or membrane thickness, was determined by the full width at half height of 36 μm-wide line profiles across equatorial confocal sections, generated using ImageJ software.

2.9. Characterization of coating/washing solutions

Supernatant solutions containing PLL*f* were analyzed by UV–Vis spectroscopy (Cary 50 Bio) following dilution in 35 mM HEPES buffer (pH 7.8) such that the $A_{495} < 1$. The A_{495} value was used to calculate the concentration of PLL*f*, using the PLL*f* extinction coefficient of 2.67 $mL \cdot cm^{-1} \cdot mg^{-1}$ described above.

Some gelling and washing solutions were analyzed for Ca^{2+} content using inductively coupled plasma-mass spectrometry (ICP-MS, PerkinElmer ELAN 6100 with ELAN software) performed by the Occupational and Environmental Health Laboratory at McMaster. Samples were prepared for ICP-MS by dilution with 1% HNO_3 (trace metal grade) to bring the calcium concentration within the calibration range of 0.2–10 ppm.

2.10. Statistics

All values are reported and graphed as mean ± standard deviation, with significant differences determined from Student's *t*-test analysis between two groups and one-way ANOVA with a Bonferroni post hoc analysis for comparison of more than two groups. Significance was determined for $p < 0.05$.

3. Results and discussion

Micropipette aspiration has been used extensively to study the mechanical properties of cells [38–40], and thin walled capsules [41–44]. It involves using a micropipette to apply a pressure differential to the wall of a captured cell or capsule, and visually measuring the length of the tongue aspirated into the pipette as a function of applied pressure differential. The cell or capsule is often modeled as a liquid droplet, or an elastic or viscoelastic solid. In the case of liquid droplets, the surface tension, T, is described by the inset of Scheme 1 and the corresponding Eq. (1), where P_1 is the pressure inside the micropipette, P_2 is the pressure of the suspending medium, R_p is the inner radius of the micropipette, R_c is the radius of the microcapsule, and x is the length of the tongue drawn into the pipette. Eq. (1) is only valid when x is less than R_p [41].

$$P_2 - P_1 = 2T\left\{\left[2x/\left(x^2 + {R_p}^2\right)\right] - [1/R_c]\right\}. \quad (1)$$

The membrane tension of liquid-filled capsules with thin, semipermeable membranes can be obtained by an application of Laplace's law, which describes the stretching deformation of a membrane caused by an applied pressure differential. This model however, does not account for any bending stresses due to finite wall thicknesses, or for the presence of a cohesive gel core that would resist deformation [41].

Cells and capsules with gel cores, are usually modeled as incompressible elastic or viscoelastic solids by applying the homogenous half-space model. Eq. (2) can be used to determine Young's modulus for such samples, provided that the inner diameter of the capillary R_p is much smaller than the diameter of the sample aspirated [47].

$$\Delta P = \left(2\pi E x/3R_p\right)\phi \quad (2)$$

Here, $\Delta P = P_2 - P_1$ is the applied pressure differential, and E is Young's modulus of the capsule. ϕ is the wall function, a term with some dependence on the capillary wall thickness. Eq. (2) requires a thin-walled pipette having a small inner diameter compared to the capsule diameter [47], and only measures the local surface modulus or requires a homogenous sample.

The present study uses aspiration capillaries with an inner diameter approximately 1/2 of the initial capsule diameter, to study the stiffness of both hydrogel beads and capsules and hence Eq. (2) cannot be strictly applied. However, the relatively large radius of the capillary is advantageous, because it provides information on the mechanical properties of the entire bead which are the main interest in capsule applications. Given the relatively large capillary inner diameter, a plot of deformation, normalized to the pipette radius $(x - x_o)/R_p$ *versus* pressure differential (ΔP), reflects a combination of core and membrane properties.

This work studies the initial **A** beads formed by gelling sodium alginate droplets with calcium chloride, as well as the **AP** and **APA** capsules formed by subsequent coatings with PLL, and finally alginate. This approach to capsule formation was originally developed by Lim and Sun [1] and remains the basis for most cell encapsulation procedures [15,16]. The term *bead* is used to reflect the gel nature of the entire as-formed **A** spheres, while with **AP** and **APA**, the term *capsule* indicates the presence of a PEC shell around the gel or liquid core.

Despite the recognition that calcium loss may occur by exchange with sodium during preparation and storage, there remain significant differences in how different laboratories prepare and handle such capsules [48,49]. One aim of this paper is to detail how subtle variations in preparation and storage conditions can influence the structure and the mechanical properties of these hydrogel beads and capsules.

3.1. Micropipette aspiration applied to calcium alginate type

Fig. 1 illustrates primary aspiration data for seven **A** beads with diameters ranging from 564 to 710 μm. These particular beads had been stored in saline, and were transferred into fresh saline just prior to testing. Fig. 1 shows a linear increase in the non-dimensional strain $(x - x_o)/R_p$ with increasing pressure differential, for each bead. The deformation $(x - x_o)$ was determined from the length of the projection into the capillary, x, minus x_o, the length of the tongue projecting into the capillary at zero pressure differential resulting from the natural curvature of the beads. x_o was determined from the x-intercept of ΔP *versus* x plots since beads could not be captured at $\Delta P = 0$. The slopes (pressure differential, ΔP, *versus* $(x - x_o)/R_p$) describe the

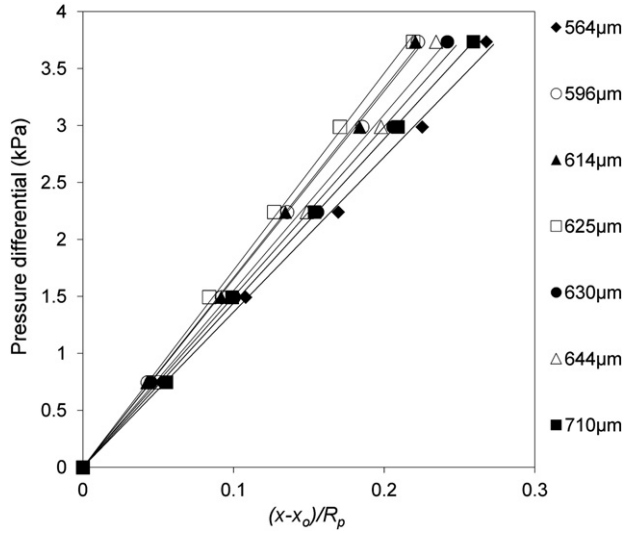

Fig. 1. Pressure differential (ΔP) versus normalized deformation $(x - x_o)/R_p$ for **A** beads with diameters from 564 to 710 μm.

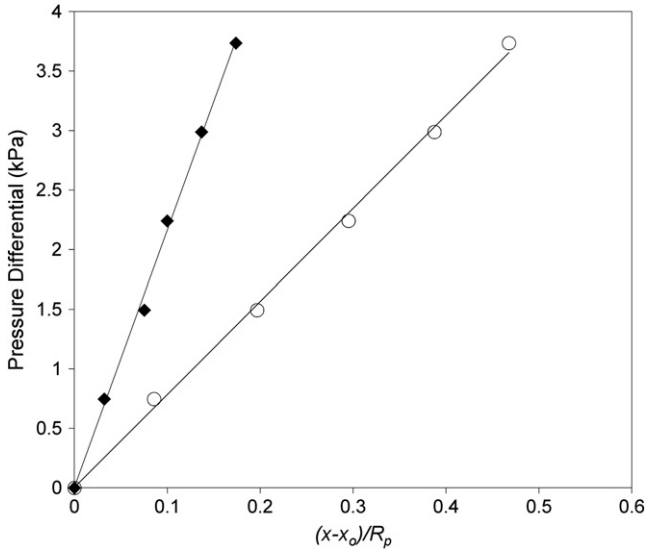

Fig. 2. Aspiration plots for individual calcium alginate beads as formed (♦) and washed three times with saline (○). The aspiration curves are linear fits to the data points.

stiffness of the beads, where the differences in the slope are attributed to random scatter in the sample stiffness rather than a function of bead size (see Fig. S1 in the Supporting information for a plot of stiffness *vs.* bead diameter). Thus, the average stiffness of these beads was measured to be 15.5 ± 1.3 kPa.

The stiffness of **A** beads and **AP** capsules, determined from this method are equivalent within experimental error for different capillaries of the same inner diameter. The *slope* of the linear aspiration curves reflects the beads' overall stiffness, which may include contributions from:

1) stretching and bending stress of the membrane during deformation [41], and
2) deformation of the gel core, including water-loss from core compression.

Data points were rejected when the projection into the pipette exceeded the inner radius of the pipette. In such cases images were collected more frequently at low pressure differentials to ensure an adequate number of data points with $x < R_p$.

Fig. 2 shows aspiration curves for **A** beads that had been treated to zero and three saline washes (one bead each). These aspiration curves show how stiffness decreases with successive saline washes, reflecting weakening of the calcium alginate gel due to calcium loss.

3.1.1. Mechanical properties of calcium alginate-based beads

The properties of the calcium alginate beads are affected by the concentration and MW of the alginate, as well as the ratio and distribution of its guluronic (G) and mannuronic acid (M) units. Higher G/M ratio alginates produce stiffer gels with better mechanical integrity [50]. Also important are the type and concentration of the gelling ion (typically Ca^{2+}, as well as Sr^{2+} or Ba^{2+}), the presence of other ions such as sodium in the gelling solution, and the gelling time and temperature. Divalent cations with higher affinities for alginate, such as Sr^{2+} and Ba^{2+} lead to formation of inhomogeneous beads (dense shell, diffuse core), while the addition of non-gelling ions such as sodium to the gelling bath, leads to beads with increased homogeneity [9,51]. Bead properties can continue to change with storage, especially due to Ca^{2+} loss [9,50,52].

Treatment of **AP** and **APA** capsules with citrate has often been done in the past to extract calcium and liquefy the cores [16,31,53]. This process will remove contributions of stiffness arising from the calcium alginate gel core and the calcium alginate portion of the shell, and leave only the PLL–alginate PEC component of the shell.

Less well appreciated is the significant effect of washing steps during preparation, on the structure and strength of the alginate-based capsules. Hsu et al. found that omitting a saline wash prior to PLL coating led to stronger **APA** capsules with denser shells and higher *in vivo* integrity [54]. Ma et al., using calcium lactate instead of calcium chloride in their gelling bath, and omitting washing with CHES ((N-cyclohexyl-) 2-aminoethanesulfonic acid) solution after PLL coating, obtained more robust capsules, as determined by the percentage of intact capsules after explantation [24].

In this work, the calcium alginate beads were prepared by gelling a 1% solution of Pronova UP MVG alginate in a bath containing 100 mM $CaCl_2$ and 77 mM NaCl. The alginate solution had a viscosity of about 200–250 cP, which is thought to be ideal for bead preparation [55]. The gelling solution contains sodium chloride at concentrations often used to generate “homogeneous” beads, with less pronounced core–shell morphology [15,16,51,56].

All solution changes were carried out using volume ratios of settled beads to new solution of 3:10. The initial gelling bath contains an excess of Ca^{2+} to alginic acid units (12-to-24-fold depending on amount of alginate gelled), and ICP-MS analysis of the gelling bath after bead formation revealed little change in the Ca^{2+} concentration. The subsequent transfer into saline reduces the calcium concentration from 100 mM to about 20 mM, reflecting a roughly 1:4 ratio of solution remaining in interstitial and pore volume in the settled beads, to new solution.

3.1.2. Effect of gelling time and temperature on stiffness of **A** beads

One common variable in the literature is the total gelling time of **A** beads, comprised of the time needed to form a batch of beads plus an additional 5–30 min in gelling bath to allow the last-formed beads to cure [50]. Longer exposure to the gelling solution can further strengthen the gel, but may be detrimental to encapsulated cells. Velings reported that at least 10 h is needed to fully stabilize calcium alginate beads stored in 50–330 mM calcium chloride solutions containing a total ionic strength of 1 M adjusted by addition of sodium chloride [57].

The **A** beads in this study were prepared during 10 to 20 min of extrusion time and stored in this initial gelling bath for an additional 10 min. They were then transferred to a fresh gelling solution for 10 min, and finally transferred into saline and stored at 4 °C.

Fig 3 shows an increase in stiffness of the resulting **A** beads from 13.2 ± 0.3 kPa for as-formed beads, to a plateau of about 34.4 ± 2.0 kPa after 500 h. This slow curing may involve additional crosslinking due to the approximately 20 mM Ca^{2+} still present in the

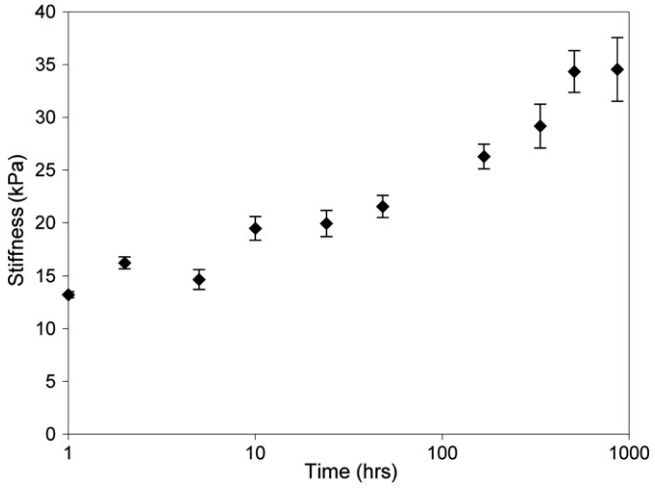

Fig. 3. Stiffness of **A** beads during storage in the first saline wash at 4 °C. Stiffness was measured at 20 °C.

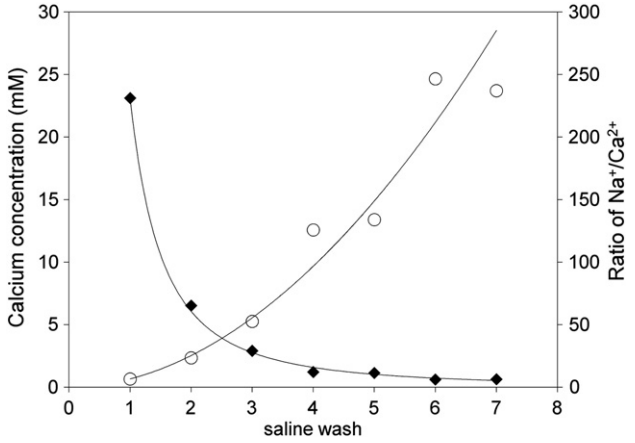

Fig. 4. $[Ca^{2+}]$ and $[Na^{+}]/[Ca^{2+}]$ in supernatant during successive saline washes of **A** beads. (♦): $[Ca^{2+}]$; (○): $[Na^{+}]/[Ca^{2+}]$.

saline storage solution, as well as annealing of existing calcium alginate crosslinks facilitated by the sodium chloride present [56,57].

Serp et al. found that heating **A** beads in 11 mM Ca^{2+} led to smaller, denser, and stiffer beads, with these effects becoming more pronounced as the temperature was increased from 50 to 130 °C [58]. Temperatures used for **A** beads containing cells usually just range from 4 to 37 °C [59–61].

To explore the effect of temperature on curing behavior in this more narrow temperature range, **A** beads washed once with saline were stored at 4, 20 and 40 °C, and their stiffness monitored over one week. The stiffness of all beads increased with time as expected from Fig. 3, with a negligibly higher curing rate at higher temperatures (see Fig. S2 in the Supporting information).

3.1.3. Effect of additional saline washes on stiffness and swelling of **A** *beads*

Additional wash cycles with saline should further reduce the Ca^{2+} concentration in the supernatant and cause Ca^{2+} loss from the beads in exchange for sodium, leading to both swelling and decreased stiffness. Bead swelling during saline washes is often used as a measure of the stability of alginate-based beads and capsules [4,24].

Serp et al. observed no swelling of calcium alginate beads when $[Na^{+}]/[Ca^{2+}]$ in solution was less than 20, though changes to mechanical properties were already noticed at $[Na^{+}]/[Ca^{2+}]$ greater than 5 [62]. Similarly, two other groups reported swelling of high G calcium alginate beads for $[Na^{+}]/[Ca^{2+}]$ ratios exceeding 20 [63] or 30 [28], and found this ratio to vary with alginate composition (G/M ratio) [28,63].

ICP-MS was used in the present work to measure $[Ca^{2+}]$ in the supernatant following successive saline washes of **A** beads, using 3:10 volume ratios of settled beads to saline wash solution.

Fig. 4 shows $[Ca^{2+}]$ dropping rapidly from 100 mM in the gelling bath to 2.9 mM after the third wash, and then descending more slowly as bound Ca^{2+} was released into the supernatant.

Fig. 5 compares the diameter and stiffness during these successive saline washes. It had previously been shown that calcium alginate gels stored in saline containing 1.8 mM $CaCl_2$ and 0.15 M NaCl decreased in strength over the first 15 h [11]. As a result, beads were stored for a minimum of 20 h after each saline wash before carrying out these measurements.

The first saline wash did not affect stiffness or bead diameter. This appears to be consistent with previous data by Morch et al., carried out using slightly different washing protocols [9]. As mentioned above, the presence of about 20 mM of calcium in the first saline wash is sufficient to maintain the gel strength.

After the second saline wash, the calcium concentration is reduced to ~6.5 mM ($[Na^{+}]/[Ca^{2+}]$ ratio of 24) and the stiffness decreased significantly compared to the starting alginate bead ($p < 0.05$ by Student's *t*-test). In contrast, the bead diameter only started to increase at the third saline wash compared to the starting mean diameter ($p < 0.001$), where the $[Na^{+}]/[Ca^{2+}]$ exceeded 30. Stiffness decreased and diameter increased until the seventh wash, at which point the beads were at the brink of failure and could not be aspirated without rupture.

These data suggest that aspiration is a much more sensitive probe for bead strength and calcium loss, than measurement of bead diameters.

In contrast to the above saline-washed **A** beads, **A** beads washed with gelling bath showed slight increases in stiffness (see Fig. S3 in the Supporting information), likely because of ongoing annealing of the gel, rather than further calcium uptake. The average stiffness (31 ± 6 kPa) after two or more washes (48 h in 100 mM calcium chloride) was greater than or equal to the stiffness of 34 ± 2 kPa reached after approximately 500 h in 20 mM calcium chloride (Fig. 3).

3.2. Stiffness of **AP** *capsules as a function of coating protocol*

The calcium alginate beads (**A**) used in cell encapsulation are usually coated with a polycation such as PLL. The resulting PLL–alginate PEC shell reduces capsule permeability, and increases capsule mechanical stability. The nature of this PEC shell depends on G/M ratio, calcium alginate porosity, PLL MW and concentration [4,24,52], and ionic strength and type of ions present in the medium [4]. Lower

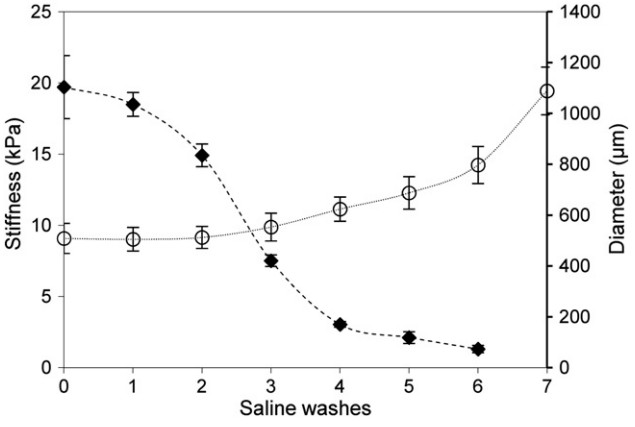

Fig. 5. Stiffness (♦) and diameter (○) of **A** beads as function of the number of saline washes.

MW PLL can penetrate more deeply into the bead to form a thicker shell, while higher MW PLL leads to thinner shells. Similarly, increasing the PLL coating time and concentration can increase the thickness of the membrane [24,49], the amount of PLL bound [4] and the strength of the capsule [52].

Vandenbossche et al. studied the MW cut-off and PLL distribution in **APA** capsules as a function of PLL coating time and concentration and suggested that in order to reduce variability between batches, PLL should be allowed to react with calcium alginate until completion, *e.g.* for 30 min at 40 °C, for a PLL concentration of 0.1% (w/v) [48]. With an eye to maximize eventual cell viability, a more conservative coating protocol was used in the present study (0.05% PLL for 6 min at 4 °C) [15,16,64–67]. Coating conditions were kept constant, and stiffness measured by aspiration was used to determine the effects of different washing protocols after PLL coating.

3.2.1. Effect of washing solution on **AP** capsules

Different protocols in the literature describe washing capsules with saline [5,48,51,54,68–70], or gelling bath [15,16], following PLL coating. To the best of our knowledge the effect of calcium on PLL distribution and associated mechanical properties in **AP** capsules has not yet been reported. Calcium alginate beads will bind more chitosan from coating solutions containing calcium chloride, rather than saline. This effect was attributed to calcium specifically rather than differences in ionic strength and thought to be due to a greater porosity of the alginate beads facilitating chitosan loading [71].

The present study hence explores the effect of different saline and calcium chloride treatments, on swelling, stiffness and PLL distribution of **AP** and **APA** capsules.

3.2.2. Effect of calcium exposure on **AP** capsules

AP capsules were washed with a) saline for 2 min, b) gelling solution for 2 min, or c) gelling solution for 2 h, before being transferred to saline. The three types of capsules are denoted as $\mathbf{AP^{SS}}$, $\mathbf{AP^{GS}_{2\,m}}$ and $\mathbf{AP^{GS}_{2\,h}}$, respectively, where SS, $GS_{2\,m}$ and $GS_{2\,h}$ denote their washing histories.

UV/Vis analysis of the combined coating and first washing supernatants showed that all three capsules bound similar amounts (84–86%) of the PLL*f* from the coating solutions.

Fig. 6a compares the stiffness of the three capsules. The $\mathbf{AP^{SS}}$ capsules have a stiffness (23 ± 2 kPa) comparable to those of the **A** beads (25 ± 2 kPa after 24 h of storage). It appears that the formation of the PEC shell in the $\mathbf{AP^{SS}}$ capsules offsets any weakening of the calcium alginate gel upon exposure to saline during coating and washing. The $\mathbf{AP^{GS}_{2\,m}}$ (42 ± 4 kPa) and $\mathbf{AP^{GS}_{2\,h}}$ (45 ± 4 kPa) were significantly stiffer than $\mathbf{AP^{SS}}$ capsules which is mainly attributed to these capsules retaining the strength of their calcium alginate gel cores. ICP-MS revealed that the $\mathbf{AP^{SS}}$ capsule experienced Ca^{2+} levels of about 2.5 mM in the second saline wash. In contrast, the $\mathbf{AP^{GS}_{2\,m}}$ and $\mathbf{AP^{GS}_{2\,h}}$ capsules have 20 mM Ca^{2+} in their storage solution, and hence the strength of the calcium alginate gel is maintained or even increased by extended curing.

The capsule diameters are consistent with the differences in stiffness showing marginally larger mean diameter for $\mathbf{AP^{SS}}$ capsules (544 ± 45 μm) compared to the $\mathbf{AP^{GS}_{2\,m}}$ and $\mathbf{AP^{GS}_{2\,h}}$ capsules (524 ± 39 μm and 518 ± 38 μm, respectively). While the differences in diameter between the $\mathbf{AP^{SS}}$ capsules and either $\mathbf{AP^{GS}}$ capsule ($p < 0.01$ by ANOVA) are statistically significant, the absence of overlap of the standard deviations in stiffness measurements illustrates the greater signal/noise of the aspiration data.

As mentioned above, stiffness measurements using intermediate diameter capillaries reflect properties of both gel cores and PEC shell. To distinguish between these contributions, the three capsule types were treated with sodium citrate to remove Ca^{2+} and liquefy the core.

The citrate-treated $\mathbf{AP^{SS}}$ capsules (Fig. 6a) showed only a moderate further decrease in stiffness, attributed to removal of bound Ca^{2+} from the core and shell.

In contrast, citrate treatment led to a large decrease in stiffness for both $\mathbf{AP^{GS}}$ capsules, reflecting the large role of calcium in stiffening these capsules before citrate treatment. Of special interest is that both types of $\mathbf{AP^{GS}}$ capsules had lower stiffness than $\mathbf{AP^{SS}}$ capsules following citrate treatment (Fig. 6a), indicating that post-PLL gelling bath washes may only temporarily strengthen the capsules. These results are consistent with recent analogous observations where PLL–alginate capsule walls were found to be softer than those of calcium alginate [34].

While the relative degree of capsule swelling is often used to assess capsule strength, swelling caused by citrate treatment of these particular capsules proved to be an unreliable indicator of relative capsule strength. The three types of capsules, swelled by small, and similar amounts (about 15–20 ± 10%) upon citrate treatment, while showing quite different capsule stiffness ($p < 0.01$ for all citrate treated **AP** capsules).

Confocal microscopy revealed that gelling bath washes allow the initially bound PLL*f* to redistribute further into the capsules (Fig. 7). While in $\mathbf{AP^{SS}}$ capsules the PLL*f* shell was 9.2 ± 0.9 μm thick, washing with gelling bath led to PLL*f* shell thicknesses of 26 ± 2 μm for $\mathbf{AP^{GS}_{2\,m}}$ and 46 ± 4 μm for $\mathbf{AP^{GS}_{2\,h}}$. Subsequent citrate-treatment caused little change in PLL*f* shell thicknesses, at 10 ± 1, 27 ± 1 and 51 ± 3 μm, respectively, lending confidence that aspiration measurements of these hollow capsules reveal the contribution of the PEC shell to the overall stiffness of the earlier, composite capsules that still had calcium alginate gel components in the core and shell contributing to stiffness.

Previous studies have observed the migration of polycations in capsules and found that it can be facilitated by the presence of

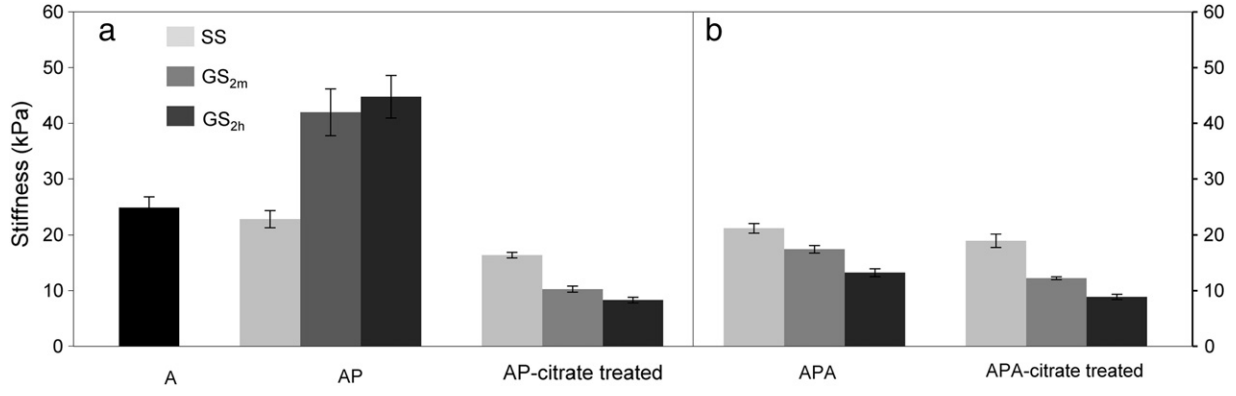

Fig. 6. The effect of different washing protocols on the stiffness of a) **AP** and b) **APA** capsules, both as formed, and following treatment with citrate to fully dissolve the calcium alginate cores. SS, $GS_{2\,m}$ and $GS_{2\,h}$ correspond to washing in saline (2 min) or gelling bath wash for (2 min or 2 h), respectively, followed by storage in saline.

divalent metal ions such as Ca^{2+}. Strand et al. noticed slow changes to PLL distribution in **AP** capsules during storage in saline containing 1 mM $CaCl_2$, leading to a doubling of the shell thickness over two weeks, with no further changes over two years [51]. Gåserød et al. found dramatic differences in the rate, location and extent of chitosan binding, depending on the Ca^{2+} content of the coating solution [71,72]. Higher [Ca^{2+}] in the coating solution led to increased in-diffusion, more chitosan bound and greater capsule strength. While higher ionic strength was thought to facilitate chitosan in-diffusion, the rate and extent of chitosan binding were greater in the presence of $CaCl_2$ than for NaCl solutions of the same ionic strength. Enhancement of cooperative Ca^{2+}–alginate binding, sometimes referred to as egg box structures, and the resulting increased porosity, was believed to be important.

Thu et al. reported that the presence of 12 mM Ca^{2+} or Sr^{2+} in the supernatant caused the release of PLL from **AP** capsules into the surrounding solution during three weeks of storage [4]. It appears that most of the PLL*f* migration in the capsules studied here takes place within the hydrogel rather than into the supernatant, as confirmed by the presence of only trace amounts of PLL*f* in washing solutions determined by UV–Vis analysis.

In the current work, all three types of capsule bind similar amounts of PLL but the different washing procedures cause different radial distributions. The high charge density of PLL is thought to lead to a "hit and stick" mechanism, causing PLL to initially bind preferentially to surface regions [4,73]. Higher ionic strength and, in particular, Ca^{2+} in the washing solution, can weaken the interactions between PLL and alginate, allowing PLL to diffuse further into the gel. This results in thicker but lower density PEC shells that are less stiff once the calcium alginate component is removed by citrate or, equivalently, multiple saline washes as described below. In addition to affecting capsule strength, the differing shell morphologies might influence the permeability and biocompatibility of the membranes. The sensitivity of capsule structure to slight variations in preparation details (*e.g.*, washing) may help to explain why capsules made with apparently similar procedures can perform quite differently.

The rate at which the PLL*f* moved further into the **AP** capsules was examined by tracking the shell thickness and stiffness over time for capsules stored in gelling bath (100 mM Ca^{2+}, 77 mM Na^{+}) and first saline wash (~20 mM Ca^{2+}, 154 mM Na^{+}) (Fig. 8), respectively. The shells of capsules stored in ~20 mM Ca^{2+} thicken from about 25 to 30 μm over 30 min, and then more slowly to 35 μm after 13 h. The capsules stored in 100 mM Ca^{2+} show a much faster increase in shell thickness, reaching 75 μm after 18 h.

The above **AP** capsules, stored in 100 mM Ca^{2+} for 2 min to 18 h, were treated with citrate to liquefy the core, and then tested by aspiration. Citrate-treatment is used here to mimic the replacement of calcium with sodium during multiple saline washes, or indeed during incubation and implantation. Fig. 9 shows that the PEC shells become both thicker and more compliant with increasing storage time in 100 mM Ca^{2+}.

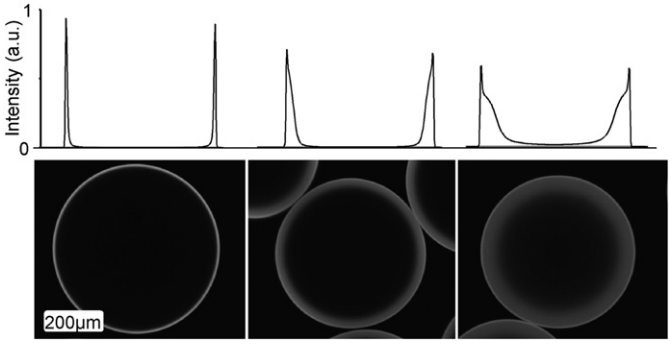

Fig. 7. Line profiles (top) and equatorial confocal images (bottom) showing the distribution of PLL*f* in $\mathbf{AP^{SS}}$ (left), $\mathbf{AP^{GS}_{2\,m}}$ (middle) and $\mathbf{AP^{GS}_{2\,h}}$ (right) capsules.

These results confirm that storage in gelling bath following PLL coating can increase short-term gel stiffness, but can compromise long-term strength of the capsules, by weakening the PLL–alginate PEC shell that is responsible for long-term integrity.

As mentioned above, calcium alginate gels weaken when exposed to saline solutions with [Ca^{2+}] of ~6.5 mM. A similar process will occur *in vivo* because of the low serum Ca^{2+} levels of about 1 mM. Both treatments with chelating agents such as citrate, and exposure to saline, are often used to mimic this process. Fig. 10 compares the stiffness for $\mathbf{AP^{GS}_{2\,h}}$ capsules treated using both methods. The resulting capsules showed increasing compliance with successive saline washes, until after six washes the stiffness levels off at a value corresponding to that of the citrate-treated **AP** capsules. These results show the rapid weakening of the gel core that occurs in solutions with low calcium levels and demonstrate that the alginate–PLL PEC shell is responsible for the long-term strength of such capsules.

$\mathbf{AP^{GS}_{2\,h}}$ capsules treated with citrate or seven saline washes experienced 18 and 6% swelling, respectively, even though both treatments lead to a three-fold decrease in stiffness (Fig. 10). This again highlights the ability of aspiration to detect changes in mechanical properties despite a comparative lack of swelling.

3.3. **APA** *capsules: The effect of the final alginate coating*

A final coating of alginate is often applied to **AP** capsules to improve the biocompatibility by covering the PLL, however, there is debate about the need for this step [4,5]. The effect of the final alginate coating on the mechanical and structural properties of **AP** capsules was hence examined by aspiration, optical and confocal microscopy.

$\mathbf{AP^{SS}}$, $\mathbf{AP^{GS}_{2\,m}}$ and $\mathbf{AP^{GS}_{2\,h}}$ beads were coated with 0.03% sodium alginate for 4 min to form the corresponding $\mathbf{AP^{SS}A}$, $\mathbf{AP^{GS}_{2\,m}}$A and $\mathbf{AP^{GS}_{2\,h}}$A beads, respectively. These were washed once with saline and stored in a second saline solution for 24 h before testing.

The stiffness of these three types of **APA** capsules differs significantly (Fig. 6b) with $\mathbf{AP^{SS}A}$ capsules stiffer than $\mathbf{AP^{GS}A}$ capsules ($p < 0.01$ of all **APA** capsule types). $\mathbf{AP^{SS}}$ capsules showed no apparent change after coating with alginate ($p > 0.05$), while both types of $\mathbf{AP^{GS}A}$ capsules were substantially weaker than their $\mathbf{AP^{GS}}$ precursors ($p < 0.01$).

Exposure to the final alginate solution and subsequent saline washes apparently causes significant loss of Ca^{2+} from the $\mathbf{AP^{GS}}$ capsules. In contrast, $\mathbf{AP^{SS}}$ beads, which already had little core gel strength prior to the final alginate coating, show little change in this step. Once the gel in the core is weakened by Ca^{2+} loss and the contribution of the shell to capsule strength becomes more important, the less diffuse shells of $\mathbf{AP^{SS}}$ capsules compared to $\mathbf{AP^{GS}}$ leads to greater stiffness.

It was found that the $\mathbf{AP^{GS}A}$ capsules have a slightly thinner PEC membranes compared to their $\mathbf{AP^{GS}}$ precursors (19 ± 1 μm and 36 ± 3 μm *vs.* 26 ± 2 μm and 46 ± 4 μm for $\mathbf{AP^{GS}_{2\,m}}$A and $\mathbf{AP^{GS}_{2\,h}}$A respectively), likely because the **APA** capsules have less exposure to significant Ca^{2+} concentrations. ICP-MS showed 20 mM Ca^{2+} in the $\mathbf{AP^{GS}_{2\,m}}$ supernatant, compared to 2 mM in the $\mathbf{AP^{GS}_{2\,m}}$A supernatant,

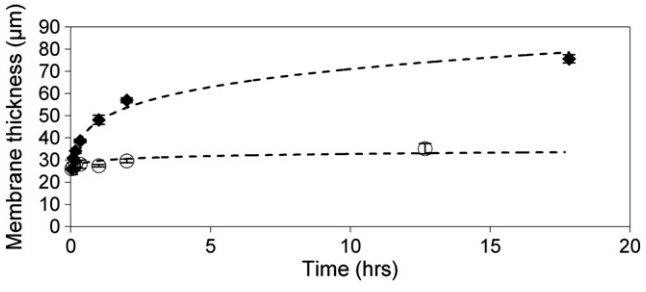

Fig. 8. Thickness of PLL*f* shell as function of storage time in (♦) gelling bath ([Ca^{2+}] = 100 mM) or (○) saline ([Ca^{2+}] = 20 mM).

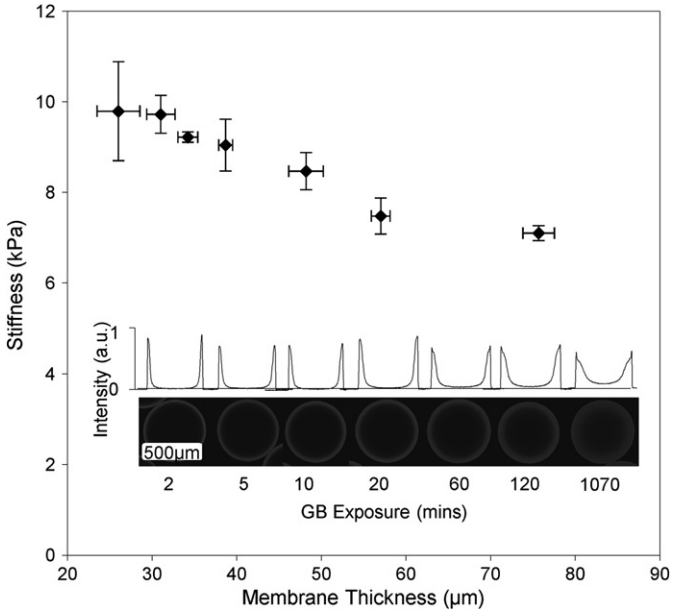

Fig. 9. Stiffness of citrate-treated **AP** capsules *versus* membrane thickness, for **AP** beads stored in gelling solution for 2 min to 18 h. The inset shows the corresponding confocal images and line profiles, before citrate treatment.

allowing continuing PLL in-diffusion in the **AP$^{GS}_{2\ m}$** capsules during storage, in contrast to the **AP$^{GS}_{2\ m}$A** capsules. Thus, coating with alginate can reduce calcium levels below those needed for further PLL in-diffusion, and thus indirectly affects PLL distribution in the **AP$^{GS}_{2\ m}$A** capsules by stopping PLL migration during storage.

Washing with a calcium-containing solution such as gelling bath following PLL coating has been done in the past to ensure a highly crosslinked gel core. It can also increase the amount of surface alginate bound to the capsule surface. This is thought to be due to the creation of an outer calcium alginate gel layer, formed using calcium escaping from the core of the capsule. However, this surface gel is not stable and about 80% was lost after 24 h of storage in saline, presumably due to calcium loss [4]. Thus, modifying **APA** capsule formation procedures can result in structural changes to the PEC shell and should be acknowledged.

3.3.1. *Effect of citrate treatment on* **APA** *capsules*

All three types of **APA** capsules were treated with citrate to dissolve any residual calcium alginate gel and determine the effect, if any, of the final layer of alginate on PEC shell stiffness. **AP^{SS}A** capsules showed a small change in stiffness after citrate treatment (Fig. 6b), indicating the presence of at most a weak gel core in the precursor capsules. Citrate treatment gave a more pronounced decrease in stiffness for **AP$^{GS}_{2\ m}$A** and **AP$^{GS}_{2\ h}$A** capsules (Fig. 6b), reflecting the presence of more gel in these cores ($p < 0.05$ on respective **APA** capsules before and after citrate treatment).

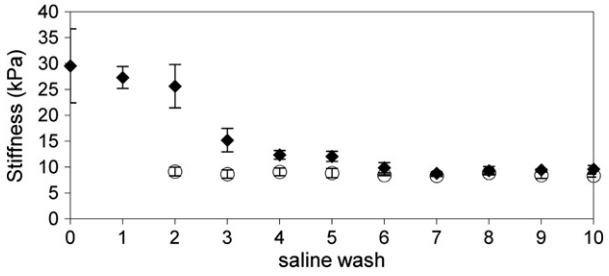

Fig. 10. Stiffness for (♦) untreated and (○) citrate-treated **AP$^{GS}_{2\ h}$** capsules as a function of saline washes.

AP^{SS}A diameters increased by 3% after citrate treatment compared to 13% for both **AP$^{GS}_{2\ m}$A** and **AP$^{GS}_{2\ h}$A** capsules, consistent with more calcium crosslinking in the gel cores for the **AP^{GS}A** capsules. The earlier loss of Ca^{2+} from **AP^{SS}A** capsules may also allow some alginate to escape from the capsules, reducing the osmotic pressure experienced during subsequent citrate treatment.

Capsules stored in their original saline supernatant show little change to the mechanical properties over a period of 6 weeks (Fig. 11). It is worth noting that any initial differences in strength between the **AP** and **APA** membranes within a capsule type tended to disappear with time (see Fig. 11), suggesting slow restructuring of the PEC membrane. The final alginate coat hence seems to not significantly contribute to the mechanical properties of **APA** capsules.

The situation may be more complex *in vivo* where encapsulated cells and the host may deposit materials, both within the capsules, and on the capsule surface. These biological processes will themselves be sensitive to the composition of the capsule. A recent study by Gardner et al. [74] found that **APA** capsules explanted after six weeks in mice were stronger than the initial capsules or those that had been incubated for six weeks *in vitro* as measured by a chemical challenge (citrate/high pH). This behavior was attributed to the deposition of cells and proteins on the outer capsule surface.

Preliminary aspiration experiments with these same capsules conducted during the current work indeed revealed that they had become stronger (stiffer) during implantation. **APA** capsules (empty or cell containing) showed an increase in stiffness after six weeks of implantation while control **APA** capsules incubated *in vitro* showed little change in stiffness. The measurements on explanted capsules were complicated by fibrotic overgrowth. Some capsules showed a large degree of fibrotic overgrowth and only capsules with minimal cellular deposits were tested. In addition, a poly(ethylene oxide) coated capillary was used to reduce interactions between protein and cellular deposits on the capsules, and the micropipette tip. We are currently

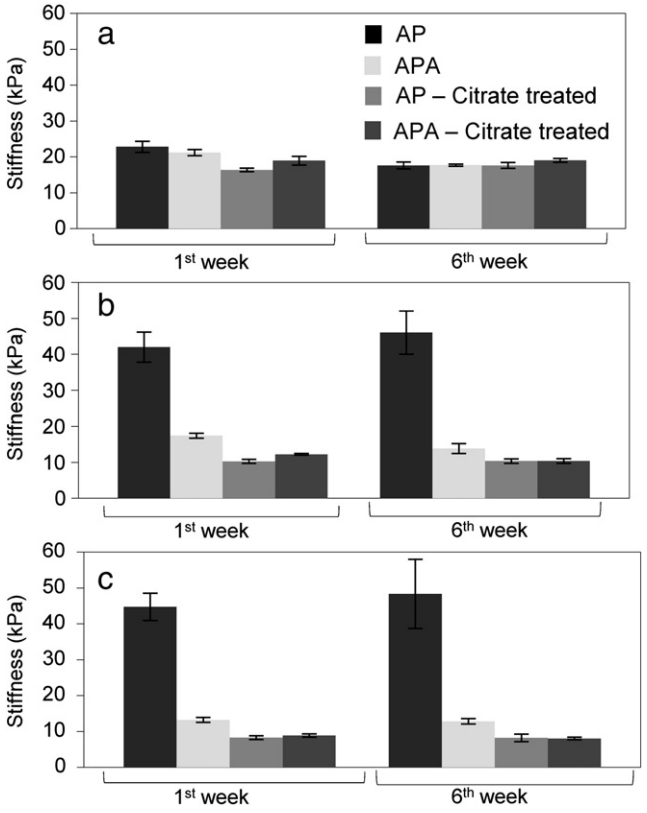

Fig. 11. Stiffness of untreated and citrate-treated **AP** and **APA** capsules during the first and sixth week of storage for a) **AP^{SS}A**, b) **AP$^{GS}_{2\ m}$A** and c) **AP$^{GS}_{2\ h}$A**.

developing cross-linked capsules with improved anti-fouling properties, and will carry out further studies on these in the future.

The current work illustrates that aspiration can serve as a rapid and sensitive tool for revealing changes to the capsule surface both *in vitro* and in biological environments. Overall, the present work may help our understanding of the complex behavior of such hydrogel capsules throughout their lifetime (preparation, coating, implantation), and may serve as a starting point for further, cell and animal-based studies.

4. Conclusion

Micropipette aspiration is a useful tool for understanding the mechanical properties of **A**, **AP** and **APA** beads and capsules, providing sensitivity in measurements yet being a rapid and simple technique. The calcium alginate core provides most of the initial mechanical strength in these hydrogels, while the PEC membrane dominates long-term stability, due to calcium loss from **AP** and **APA** capsules. The mechanical properties of this membrane depends on the coating process in several ways: gelling bath washes following the PLL deposition redistributes this polycation further into the capsule, resulting in a thicker, and, at least at the present PLL concentrations, more compliant PEC membrane. The final alginate coating speeds calcium loss from the gel core, but does not seem to affect final membrane mechanical properties.

Supplementary data to this article can be found online at http://dx.doi.org/10.1016/j.msec.2013.06.033.

Acknowledgments

We would like to thank the Natural Sciences and Engineering Research Council of Canada (NSERC) for funding, and Kevin Ferguson of OEHL at McMaster University for determination of Ca^{2+} content by ICP-MS.

References

[1] F. Lim, A.M. Sun, Microencapsulated islets as bioartificial endocrine pancreas, Science 210 (1980) 908–911.
[2] T. Yasuhara, T. Shingo, K. Muraoka, M. Kameda, T. Agari, Y.W. Ji, H. Hayase, C.V. Borlongan, I. Date, Neurorescue effects of VEGF on a rat model of Parkinson's disease, Brain Res. 1053 (2005) 10–18.
[3] C.J.D. Ross, L. Bastedo, S.A. Maier, M.S. Sands, P.L. Chang, Treatment of a lysosomal storage disease, mucopolysaccharidosis VII, with microencapsulated recombinant cells, Hum. Genet. Ther. 11 (2000) 2117–2127.
[4] B. Thu, P. Bruheim, T. Espevik, O. Smidsrød, P. Soon-Shiong, G. Skjåk-Bræk, Alginate polycation microcapsules. 1. Interaction between alginate and polycation, Biomaterials 17 (1996) 1031–1040.
[5] S.K. Tam, S. Bilodeau, J. Dusseault, G. Langlois, J.P. Hallé, J.H. Yahia, Biocompatibility and physicochemical characteristics of alginate–polycation microcapsules, Acta Biomater. 7 (2011) 1683–1692.
[6] B.L. Strand, L. Ryan, P.I. Veld, B. Kulseng, A.M. Rokstad, G. Skjåk-Bræk, T. Espevik, Poly-L-lysine induces fibrosis on alginate microcapsules via the induction of cytokines, Cell Transplant. 10 (2001) 263–275.
[7] H.K. Holme, L. Davidsen, A. Kristiansen, O. Smidsrød, Kinetics and mechanism of depolymerization of alginate and chitosan in aqueous solution, Carbohydr. Polym. 73 (2008) 656–664.
[8] S. Saitoh, Y. Araki, R. Kon, H. Katsura, M. Taira, Swelling/deswelling mechanism of calcium alginate gel in aqueous solutions, Dent. Mater. J. 19 (2000) 396–404.
[9] Y.A. Mørch, I. Donati, B.L. Strand, G. Skjåk-Bræk, Effect of Ca^{2+}, Ba^{2+}, and Sr^{2+} on alginate microbeads, Biomacromolecules 7 (2006) 1471–1480.
[10] X. Wang, H.G. Spencer, Calcium alginate gels: formation and stability in the presence of an inert electrolyte, Polymer 39 (1998) 2759–2764.
[11] M.A. LeRoux, F. Guilak, L.A. Setton, Compressive and shear properties of alginate gel: effects of sodium ions and alginate concentration, J. Biomed. Mater. Res. 47 (1999) 46–53.
[12] P. de Vos, M. Bukco, P. Gemeiner, M. Navrátil, J. Švitel, M. Faas, B.L. Strand, G. Skjåk-Bræk, Y.A. Mørch, A. Vikartovská, I. Lacík, G. Kolláriková, G. Orive, D. Poncelet, J.L. Pedraz, M.B. Ansorge-Schumacher, Multiscale requirements for bioencapsulation in medicine and biotechnology, Biomaterials 30 (2009) 2559–2570.
[13] J. Dusseault, F.A. Leblond, R. Robitaille, G. Jourdan, J. Tessier, M. Ménard, N. Henley, J.-P. Hallé, Microencapsulation of living cells in semi-permeable membranes with covalently cross-linked layers, Biomaterials 26 (2005) 1515–1522.
[14] H. Chen, W. Ouyang, B. Lawuyi, S. Prakash, Genipin cross-linked alginate–chitosan microcapsules: membrane characterization and optimization of cross-linking reaction, Biomacromolecules 7 (2006) 2091–2098.
[15] F. Shen, M.A.J. Mazumder, N.A.D. Burke, H.D.H. Stöver, M.A. Potter, Mechanically enhanced microcapsules for cellular gene therapy, J. Biomed. Mater. Res. B Appl. Biomater. 90B (2009) 350–361.
[16] C.M. Gardner, N.A.D. Burke, H.D.H. Stöver, Cross-linked microcapsules formed from self-deactivating reactive polyelectrolytes, Langmuir 20 (2010) 4916–4924.
[17] R. Gugerli, E. Cantana, C. Heinzen, U. von Stockar, I.W. Marison, Quantitative study of the production and properties of alginate/poly-L-lysine microcapsules, J. Microencapsul. 19 (2002) 571–590.
[18] A.J. Engler, S. Sen, H.L. Sweeney, D.E. Discher, Matrix elasticity directs stem cell lineage specification, Cell 126 (2006) 677–689.
[19] T. Yeung, P.C. Georges, L.A. Flanagan, B.M. Miguelina, M. Funaki, N. Zahir, W. Ming, V. Weaver, P.A. Janmey, Effects of substrate and stiffness on cell morphology cytoskeletal structure, and adhesion, Cell Motil. Cytoskeleton 60 (2005) 24–34.
[20] S.Y. Tee, J. Fu, C.S. Chen, P.A. Janmey, Cell shape and substrate rigidity both regulate cell stiffness, Biophys. J. 100 (2011) L25–L27.
[21] D.E. Discher, P.A. Janmey, Y.L. Wang, Tissue cells feel and respond to the stiffness of their substrate, Science 310 (2005) 1139–1143.
[22] J.M. Van Raamsdonk, P.L. Chang, Osmotic pressure test: a simple, quantitative method to assess the mechanical stability of alginate microcapsules, J. Biomed. Mater. Res. 54 (2001) 264–271.
[23] F.A. Leblond, J. Tessier, J.P. Hallé, Quantitative method for the evaluation of biomicrocapsule resistance to mechanical stress, Biomaterials 17 (1996) 2097–2102.
[24] X. Ma, I. Vacek, A. Sun, Generation of alginate-poly-L-lysine-alginate (APA) biomicroscopies — the relationship between the membrane strength and the reaction conditions, Artif. Cells Blood Substit. Immobil. Biotechnol. 22 (1994) 43–69.
[25] X. Liu, W. Xue, Q. Lin, W. Yu, Y. Fu, X. Xiong, X. Ma, Swelling behaviour of alginate–chitosan microcapsules prepared by external gelation or internal gelation technology, Carbohydr. Polym. 56 (2004) 459–464.
[26] M. Lekka, D. Sainz-Serp, A.J. Kulik, C. Wandrey, Hydrogel microspheres: influence of chemical composition on surface morphology, local elastic properties, and bulk mechanical characteristics, Langmuir 20 (2004) 9968–9977.
[27] K. Yamagiwa, T. Kozawa, A. Ohkawa, Effects of alginate composition and gelling conditions on diffusional and mechanical properties of calcium–alginate gel beads, J. Chem. Eng. Jpn 28 (1995) 462–467.
[28] A. Martisen, G. Skjåk-Bræk, O. Smidsrød, Alginate as immobilization material. 1. Correlation between chemical and physical-properties of alginate gel beads, Biotechnol. Bioeng. 33 (1989) 79–89.
[29] M. Mancini, M. Moresi, R. Rancini, Mechanical properties of alginate gels: empirical characterisation, J. Food Eng. 39 (1999) 369–378.
[30] C.X. Wang, C. Cowen, Z. Zhang, C.R. Thomas, High-speed compression of single alginate microspheres, Chem. Eng. Sci. 60 (2005) 6649–6657.
[31] M. De Castro, G. Orive, R.M. Hernández, A.R. Gascón, J.L. Pedraz, Comparative study of microcapsules elaborated with three polycations (PLL, PDL, PLO) for cell immobilization, J. Microencapsul. 22 (2005) 303–315.
[32] E.S. Chan, T.K. Lim, W.P. Voo, R. Pogaku, T.B. Tey, Z. Zhang, Effect of formulation of alginate beads on their mechanical behavior and stiffness, Particuology 9 (2011) 228–234.
[33] S. Leick, S. Henning, P. Degen, D. Suter, H. Rehage, Deformation of liquid-filled calcium alginate capsules in a spinning drop apparatus, Phys. Chem. Chem. Phys. 12 (2010) 2950–2958.
[34] S. Leick, A. Kemper, H. Rehage, Alginate/poly-L-lysine capsules: mechanical properties and drug release characteristics, Soft Matter 7 (2011) 6684–6694.
[35] V.B. Nguyen, C.X. Wang, C.R. Thomas, Z. Zhang, Mechanical properties of single alginate microspheres determined by microcompression and finite element modeling, Chem. Eng. Sci. 64 (2009) 821–829.
[36] L. Zhao, Z. Zhang, Mechanical characterization of biocompatible microspheres and microcapsules by direct compression, Artif. Cells Blood Substit. Immobil. Biotechnol. 32 (2004) 25–40.
[37] A. Rehor, L. Canaple, Z. Zhang, D. Hunkeler, The compressive deformation of multicomponent microcapsules: influence of size, membrane thickness, and compression speed, J. Biomater. Sci. Polym. Ed. 12 (2001) 157–170.
[38] R.M. Hochmuth, Micropipette aspiration of living cells, J. Biomech. 53 (2000) 15–22.
[39] W.R. Jones, H. Ping Ting-Beall, G.M. Lee, S.S. Kelley, R.M. Hochmuth, F. Guilak, Alterations in the Young's modulus and volumetric properties of chondrocytes isolated from normal and osteoarthritic human cartilage, J. Biomech. 32 (1999) 119–127.
[40] M. Sato, D.P. Theret, L.T. Wheeler, N. Ohshima, R.M. Nerem, Application of the micropipette technique to the measurements of cultured porcine aortic endothelial cell viscoelastic properties, ASME J. Biomech. Eng. 112 (1990) 263–268.
[41] A.W.L. Jay, M.A. Edwards, Mechanical properties of semipermeable capsules, Can. J. Physiol. Pharmacol. 46 (1968) 731–737.
[42] K. Olbrich, W. Rawicz, D. Needham, E. Evans, Water permeability and mechanical strength of polyunsaturated lipid bilayers, Biophys. J. 79 (2000) 321–327.
[43] H. Baumler, G. Artmann, A. Voigt, R. Mitlohner, B. Neu, H. Kiesewetter, Plastic behaviour of polyelectrolyte microcapsules derived from colloid templates, J. Microencapsul. 17 (2000) 651–655.
[44] C. Campillo, B. Pepin-Donat, A. Viallat, Responsive viscoelastic giant lipid vesicles filled with a poly(N-isopropylacrylamide) artificial cytoskeleton, Soft Matter 3 (2007) 1421–1427.
[45] S. Rosiński, G. Grigorescu, D. Lewińska, L.G. Ritzén, H. Viernstein, E. Teunou, D. Poncelet, Z. Zhang, X. Fan, D. Serp, I. Marison, D. Hunkeler, Characterization of microcapsules: recommended methods based on round-robin testing, J. Microencapsul. 19 (2002) 641–659.

[46] R.P. Haugland, Handbook of Fluorescence Probes and Research Products, Molecular Probes, ninth ed., Eugene, 2002. 55.
[47] D.P. Theret, M.J. Levesque, M. Sato, R.M. Nerem, L.T. Wheeler, The application of a homogeneous half-space model in the analysis of endothelial cell micropipette measurements, J. Biomech. Eng. 110 (1988) 190–199.
[48] P. De Vos, B.J. de Haan, R. Van Schlifgaard, Is it possible to use the standard alginate–PLL procedure for production of small capsules? Transplant. Proc. 30 (1998) 492–493.
[49] G.M. Vandenbossche, P.V. Oostveldt, J. Demeester, J.P. Remon, The molecular-weight cutoff of microcapsules is determined by reaction between alginate and polylysine, Biotechnol. Bioeng. 42 (1993) 381–386.
[50] O. Smidsrød, G. Skjåk-Bræk, Alginate as immobilization matrix for cells, Trends Biotechnol. 8 (1990) 71–78.
[51] B.L. Strand, Y.A. Morch, T. Espevik, G. Skjåk-Bræk, Visualization of alginate–poly-L-lysine-alginate microcapsules by confocal laser scanning microscopy, Biotechnol. Bioeng. 82 (2003) 386–394, (B).
[52] B. Thu, P. Bruheim, T. Espevik, O. Smidsrod, P. Soon-Shiong, G. Skjåk-Bræk, Alginate polycation microcapsules. 2. Some functional properties, Biomaterials 17 (1996) 1069–1079.
[53] A.M. Sun, G.M. O'Shea, Microencapsulation of living cells — a long-term delivery system, J. Control. Release 2 (1985) 137–141.
[54] B.R. Hsu, Y.S. Ho, S.H. Fu, Y.Y. Huang, S.C. Chiou, H.S. Huang, Membrane compactness affects the integrity and immunoprotection of alginate–poly-L-lysine–alginate microcapsules, Transplant. Proc. 27 (1995) 3227–3231.
[55] D.B. Seifert, J.A. Phillips, Production of small, monodispersed alginate beads for cell immobilization, Biotechnol. Prog. 13 (1997) 562–568.
[56] G. Skjåk-Bræk, H. Grasdalen, O. Smidsrød, Inhomogenous polysaccharide ionic gels, Carbohydr. Polym. 10 (1989) 31–54.
[57] N.M. Velings, M.M. Mestdagh, Physicochemical properties of alginate gel beads, Polym. Gels Netw. 3 (1995) 311–330.
[58] D. Serp, M. Mueller, U. von Stockar, I.W. Marison, Low-temperature electron microscopy for the study of polysaccharide ultrastructures in hydrogels. II. Effect of temperature on the structure of Ca^{2+}-alginate beads, Biotechnol. Bioeng. 79 (2002) 253–259.
[59] C. Young, P.D. Rekha, W. Lai, A.B. Arun, Encapsulation of plant growth-promoting bacteria in alginate beads enriched with humic acid, Biotechnol. Bioeng. 95 (2006) 76–83.
[60] N. Wang, G. Adams, L. Buttery, F.H. Falcone, S. Stolnik, Alginate encapsulation technology supports embryonic stem cells differentiation into insulin-producing cells, J. Biotechnol. 144 (2009) 304–312.
[61] H.L. Ma, S.C. Hung, S.Y. Lin, Y.L. Chen, W.H. Lo, Chondrogenesis of human mesenchymal stem cells encapsulated in alginate beads, J. Biomed. Mater. Res. A 64A (2003) 273–281.
[62] D. Serp, E. Cantana, C. Heinzen, U. von Stockar, I.W. Marison, Characterization of an encapsulation device for the production of monodisperse alginate beads for cell immobilization, Biotechnol. Bioeng. 70 (2000) 41–53.
[63] J. Vorlop, J. Klein, New developments in the field of cell immobilization—formation of biocatalysts by ionotropic gelation, in: F.M. Lafferty (Ed.), Enzyme Technology, Springer-Verlag, Heidelberg, 1983, pp. 219–235.
[64] M.F.A. Goosen, G.M. O'Shea, H.M. Gharapetian, S. Chou, A. Sun, Optimization of microencapsulation parameters—semipermeable microcapsules as a bioartificial pancreas, Biotechnol. Bioeng. 27 (1985) 146–150.
[65] A. Safley, H. Cui, S. Cauffiel, C. Tucker-Burden, C.J. Weber, Biocompatibility and immune acceptance of adult porcine islets transplanted intraperitoneally in diabetic NOD mice in calcium alginate poly-L-lysine microcapsules versus barium alginate microcapsules without poly-L-lysine, J. Diabetes Sci. Technol. 2 (2008) 760–767.
[66] G.M. Lee, B.O. Palsson, Simplified method of making alginate–polylysine microcapsules for hybridoma cell culture using RPMI 1640 medium, Biotechnol. Tech. 4 (1990) 341–344.
[67] H.A. Clayton, N.J.M. London, P.S. Colloby, P.R.F. Bell, R.F.L. James, The effect of capsule composition on the biocompatibility of alginate–poly-L-lysine capsules, J. Microencapsul. 8 (1991) 221–233.
[68] M.H. Ottøy, O. Smidsrød, Swelling of poly-L-lysine and chitosan-coated superswelling sodium-alginate gel beads, Polym. Gels Netw. 5 (1997) 307–314.
[69] A. King, B. Strand, A. Rokstad, B. Kulseng, A. Andersson, G. Skjåk-Bræk, S. Sandler, Improvement of the biocompatibility of alginate/poly-L-lysine/alginate microcapsules by the use of epimerized alginate as a coating, J. Biomed. Mater. Res. A 64A (2003) 533–539.
[70] H.A. Hobbs, W.F. Kendall, M. Darrabie, E.C. Opara, Prevention of morphological changes in alginate microcapsules for islet xenotransplantation, J. Investig. Med. 49 (2001) 572–575.
[71] O. Gåserød, O. Smidsrød, G. Skjåk-Bræk, Microcapsules of alginate–chitosan — I — a quantitative study of the interaction between alginate and chitosan, Biomaterials 19 (1998) 1815–1825.
[72] O. Gåserød, A. Sannes, G. Skjåk-Bræk, Microcapsules of alginate–chitosan. II. A study of capsule stability and permeability, Biomaterials 20 (1999) 773–783.
[73] G. Maurstad, Y.A. Mørch, A.R. Baush, B.T. Stokke, Polyelectrolyte layer interpenetration and swelling of alginate–chitosan multilayers studied by dual wavelength reflection interference contrast microscopy, Carbohydr. Polym. 71 (2008) 672–681.
[74] C.M. Gardner, M.A. Potter, H.D.H. Stöver, Improving covalent cell encapsulation with temporarily reactive polyelectrolytes, J. Mater. Sci. Mater. Med. 23 (2012) 181–193.